Eur. Phys. J. D **45**, 471–476 (2007)
DOI: 10.1140/epjd/e2007-00166-9

THE EUROPEAN PHYSICAL JOURNAL D

Optical properties of small silver clusters supported at MgO

V. Bonačić-Koutecký[1,a], C. Bürgel[1], L. Kronik[2], A.E. Kuznetsov[1], and R. Mitrić[1]

[1] Humboldt-Universität zu Berlin, Institut für Chemie, Brook-Taylor-Straße 2, 12489 Berlin, Germany
[2] Department of Materials and Interfaces, Weizmann Institute of Science, Rehovot 76100, Israel

Received 24 January 2007 / Received in final form 3rd April 2007
Published online 23 May 2007 –

Abstract. We present structural and optical properties of silver clusters Ag_n (n = 2, 4, 6, 8) at two model support sites of MgO, stoichiometric MgO(100) and F_S-center defect, based on density functional theory and embedded cluster model. Our results provide the mechanism responsible for the absorption and emission patterns due to the specific interaction between the excitations within the cluster and the support site which is strongly cluster size and structure dependent. We propose Ag_4 at stoichiometric site as well as Ag_2, Ag_4 and Ag_6 at F_S-center defects as good candidates for the emissive centers in the visible regime.

PACS. 31.15.Qg Molecular dynamics and other numerical methods – 31.15.Ar Ab initio calculations

1 Introduction

Small silver clusters have attracted considerable attention in a search for efficient fluorescent nanoscale materials which can be used for advancing optical data storage media [1–8], to build optical logic devices [4,5,7] and for biosensing [9,10]. Under UV- or visible light excitations silver clusters with few atoms embedded in rare gas matrices exhibit light emission [11–15]. The role of the matrix is to prevent cluster fragmentation which is observed for the free silver clusters in the gas phase. Due to almost negligible influence of rare gas matrices or helium droplets [16] on optical properties of silver clusters our previous theoretical work on absorption and emission properties of gas phase silver clusters in the nonscalable size regime provided the mechanism for excitations responsible for experimental findings [15,17,18]. We have shown that optical properties are strongly structure and size selective due to discrete molecular-like nature of such small metallic particles. After discovery that silver clusters fluoresce also at surfaces and in bioenvironment [1,10] the application aspects became evident. For example, it was recognized that observed photoactivated fluorescence upon illumination of silver-oxide films caused by formation of silver clusters can be useful for optical storage with high data capacities [1]. This can be achieved by efficient multicolour writing followed by readout via fluorescence excitation in visible [6–8]. Moreover, it was shown that small silver clusters can be used to produce single molecule like emitting diodes and optoelectronic logical gates [7].

Since the mechanism responsible for such emissive properties of clusters formed by photoreduction of silver-oxide films was not known, we have studied first optical properties of silver clusters interacting with silver-oxide support [19]. Due to Ag-Ag interaction between the cluster and the oxidic silver support, strong mixing of excitations within both subunits does not allow to distinguish the inherent cluster and support contributions and thus to unravel the mechanism for photoemission. Consequently, an ionic MgO support offers a more suitable environment for studying optical properties of supported silver clusters since the contributions from the cluster and the support can be easier distinguished. In fact, due to easy preparation the MgO support has been experimentally widely used in studies of properties of supported clusters [20]. However, the characterization of the different types of defects is still a subject of intense experimental and theoretical investigations [21–23]. Theoretical studies of noble metal clusters at MgO support have been concentrated mainly on the ground state properties in the context of catalytic activity [24–35]. The investigation of the optical properties of small gold clusters at MgO support aimed also to identify the active centers for oxidation reaction [36]. The influence of the MgO support on structures and optical transitions in copper clusters has been recently investigated [37].

Our contribution aims to reveal the mechanism responsible for absorption and emission of supported silver clusters at different model sites of MgO (stoichiometric versus F_S-center defect) and to propose size selective emissive centers. The choice of the sites has been made in order to study the influence of the surface and of the simplest oxygen vacancy on the absorption patterns of silver clusters. Therefore, we present in this contribution a comparison of optical and emissive properties of Ag_n (n = 2, 4, 6, 8) at these two different sites of MgO support based on time-dependent density functional method

[a] e-mail: vbk@chemie.hu-berlin.de

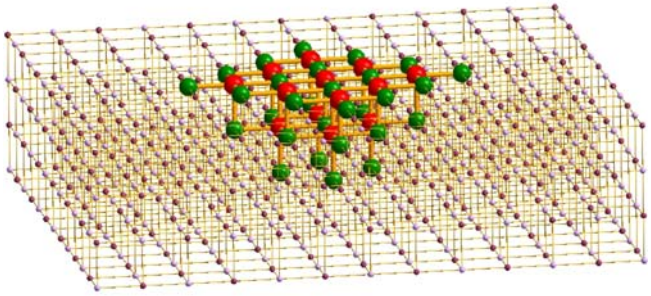

Fig. 1. (Color online) Schematic representation of the embedded cluster model for the MgO-support used to study the absorption properties of supported silver clusters. The model consists of a quantum mechanical part represented by a $Mg_{13}O_{13}(Mg^{2+})_{16}$ cluster embedded in an array of $13\times13\times10$ point charges for stoichiometric MgO(100) support. The model for the F_S-center defect is obtained by removing one O-atom.

(TDDFT). The analysis of the nature of excitations within the interacting subunits allowed us to characterize and classify the transitions as a function of the cluster size and the nature of the support site.

We wish to show that the optical properties of silver clusters are largely preserved on the stoichiometric MgO(100) surface and in principle they can act as emissive centers in different wavelength regimes provided that they are sufficiently stabilized by a relatively weak interaction with the support. In contrast, the new type of optical transitions arise for the clusters at F_S-center defects in which the interplay between excitations within the cluster and the defect can give rise to emission in the visible spectral range which is suitable for applications. This may serve as a prototype for further investigation of absorption properties of clusters at other classes of defects.

2 Computational methods

In order to describe MgO support which is of ionic nature, we use the embedded cluster approach [38]. The full quantum mechanical treatment is restricted to $Mg_{13}O_{13}$ and $Mg_{13}O_{12}$ clusters which model the stoichiometric MgO(100) surface and the F_S-center, respectively. The distant part of the electrostatic field of the support is represented by an array of point charges (PC) [20,34,39–41]. In order to avoid strong polarization by positive PC's the Mg^{2+} cations have been introduced at the boundary of the model. As a result $Mg_{13}O_{13}(Mg^{2+})_{16}$ and $Mg_{13}O_{12}(Mg^{2+})_{16}$ are embedded in a large array of PC's, e.g. $13\times13\times10$ as shown in Figure 1.

DFT method with gradient corrected Perdew-Burke-Ernzerhof (PBE) [42] functional and triple zeta plus polarization atomic basis set (TZVP) for Mg and O together with 19-electron relativistic effective core potential from the Stuttgart group [43] (19e-RECP) with corresponding AO basis set for Ag has been used to determine the ground state structural and binding properties of Ag_n clusters at the MgO support. The calculations of absorption spectra and optimization of excited state geometries of supported silver clusters were carried out using TDDFT method with PBE functional employing TZVP basis set for MgO, while for silver atoms our 11e-RECP with corresponding basis set was used [17]. This ECP was designed for accurate description of excited states of silver clusters. Due to our previous results on absorption properties of silver clusters based on more accurate and highly correlated EOM-CCSD method we were able to compare the spectra calculated by TDDFT method and obtained satisfactory agreement [17,18]. We consider optically allowed transitions and do not take into account different multiplicities. Our model is suitable for qualitative analysis of interactions between excitations within silver cluster and within the support. Structural properties have been determined by optimization of the cluster coordinates and keeping Mg and O atoms fixed for the ground electronic states in the framework of analytical gradient method. The relaxation of neighboring atoms of the F_S-center doesn't influence results significantly.

Table 1. Binding energies in eV of Ag_n clusters at MgO (100) surface and at F-center.

	Ag_n at MgO (100)	Ag_n at F-center
Ag_2	0.78	1.91
Ag_4	1.17	2.64
Ag_6	1.23	2.41
Ag_8	1.33	2.34

The presence of F_S-center or other defects under certain experimental conditions is still under debate [23,44,45]. The optical transitions in the visible regime are characteristic for several defects [23]. Notice that the location of the low energy intense transitions of the defects can be affected by the size of the model. Therefore, for quantitative purposes a systematic investigation of extended embedded model has to be carried out since the location of the low energy transitions might be affected by the choice of the model. This is out of the scope of this contribution.

3 Results and discussion

Absorption spectra for free clusters, for clusters at stoichiometric MgO(100) support and at F_S-center defects obtained for optimized structures are given for cluster size 2, 4, 6 and 8 in Figures 2–5. The binding energies at different sites are listed in Table 1 which shows that F_S-center binds stronger, as expected. The optimized structures are also shown in Figures 2–5. Extensive search for structural properties of supported clusters has been carried out. In general, perpendicularly bound clusters are considerably stronger bound than the flat ones by more than ≈0.5 eV. In the case of clusters at stoichiometric surfaces this is due to a polarization effect which is stronger for the perpendicularly bound clusters. Similarly, for the clusters at F_S-center the interaction with the orbitals of the F_S-center is stronger also for such geometrical arrangement. The results of analysis of leading excitations contributing to selected intense transitions are presented in Figures 2–5 as

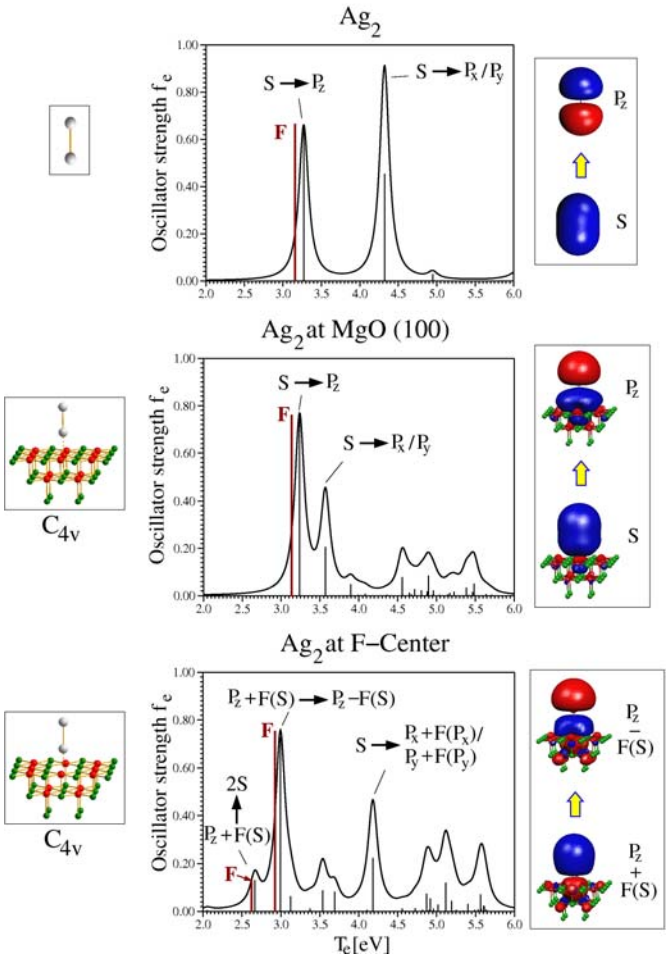

Fig. 2. (Color online) Comparison of absorption spectra for free Ag_2, Ag_2 at stoichiometric MgO(100) and Ag_2 at F_S-center defect obtained for optimized structures. The nature of characteristic excitations involved in intense transitions is assigned and the corresponding orbitals are shown. The position of the fluorescence line (red line) obtained by optimizing the geometry of the corresponding excited state is labeled by F.

well. Notice that each of the transitions is due to a linear combination of many excitations but in order to characterize their nature qualitatively the leading contributions will be used for this purpose throughout the paper. Since the energy differences between the isomers of supported clusters are considerably larger than for free clusters it is to expect that the influence of the temperature on absorption properties of supported clusters is less critical than in the case of free clusters.

Ag_2/MgO

Silver dimer is perpendicularly bound to the support at both sites as can be depicted from Figure 2. For Ag_2 at stoichiometric MgO(100) the lowest energy dominant transition located at 3.23 eV arises mainly from $S \rightarrow P_z$ (HOMO-LUMO) excitation as shown in Figure 2. The second intense transition at 3.57 eV is due to doubly degenerate $S \rightarrow P_{x,y}$ excitations. The nature of these two intense transitions is analogous to those found in a free Ag_2 dimer. However, the red shift of $S \rightarrow P_{x,y}$ type transition by 0.75 eV is due to relative lowering of the energy of the two $P_{x,y}$ orbitals with respect to the S-orbital of the supported system due to mixing with the occupied O($2p$) band. Consequently the intensity of these transitions are also reduced under the influence of the support. In contrast, the location and intensity of the lowest energy transition which is dominated by $S \rightarrow P_z$ excitation remains unchanged in supported systems. The structural relaxation in the excited state of this transition gives rise to fluorescence band origin at 3.1 eV, close to the dominant absorption band.

Binding of cluster at the F_S-center defect leads to the linear combinations of cluster and F_S-center orbitals. In the case of Ag_2 at F_S-center the HOMO is P_z + F(S), which is a P-type orbital and therefore the optically allowed excitations take place to the S- and D-type orbitals. Consequently, the two lowest energy transitions at 2.67 and 2.99 eV arise due to linear combination of excitations P_z + F(S) (P-type) $\rightarrow$ P_z – F(S) (D-type) and from P_z + F(S) $\rightarrow$ 2S as shown in Figure 2. The transition at 2.67 eV has larger contribution from P_z + F(S) $\rightarrow$ 2S excitation while the dominant transition at 2.99 eV has larger contribution from P_z + F(S) (P-type) $\rightarrow$ P_z – F(S) (D-type) excitation. These types of excitations are characteristic of the supported system and are not present in isolated Ag_2. However, the intense transition at 4.2 eV lies sufficiently high in energy since it is not influenced by the F_S-center and is therefore reminiscent of the transition in dimer. Notice that fluorescence might occur from two lowest energy transitions which are strongly influenced by the F_S-center.

Ag_4/MgO

Silver tetramer is perpendicularly bound to the stoichiometric surface and to the F_S-center of MgO as shown in Figure 3. The addition of two atoms changes the absorption pattern of supported Ag_4 cluster at MgO(100) significantly due to interaction of the orbitals which are polarized parallel to the surface. Consequently, the lowest energy transition located at 2.67 eV is due to $P_x \rightarrow D_{x^2}$ excitation and is polarized in the x-direction parallel to the surface. This transition is red shifted with respect to the analogous type in the free Ag_4 cluster as shown in Figure 3. The second intense transition at 3.95 eV is of $S \rightarrow P_z$ nature as in the free cluster, and it remains almost unchanged in energy because it is not influenced by the surface. The relaxation of excited state geometry of the lowest intense transition leads to the fluorescence line located close to the transition at 2.67 eV. Therefore, Ag_4 at the stoichiometric support is a possible candidate for emissive center in the visible range provided that it is sufficiently stabilized.

In the case of Ag_4 at F_S-center P_x + F(P_x) orbital becomes occupied. Therefore, the lowest energy transition at 2.52 eV is due to P_x + F(P_x) $\rightarrow$ D_{x^2} + F(P_z) (P-type $\rightarrow$ D-type) excitation as shown in Figure 3. This transition is red shifted by 0.5 eV with respect to analogous type of transition in free Ag_4 due to linear combination with F_S-center orbital. Notice that in this case the lowest intense transition is also well isolated from other

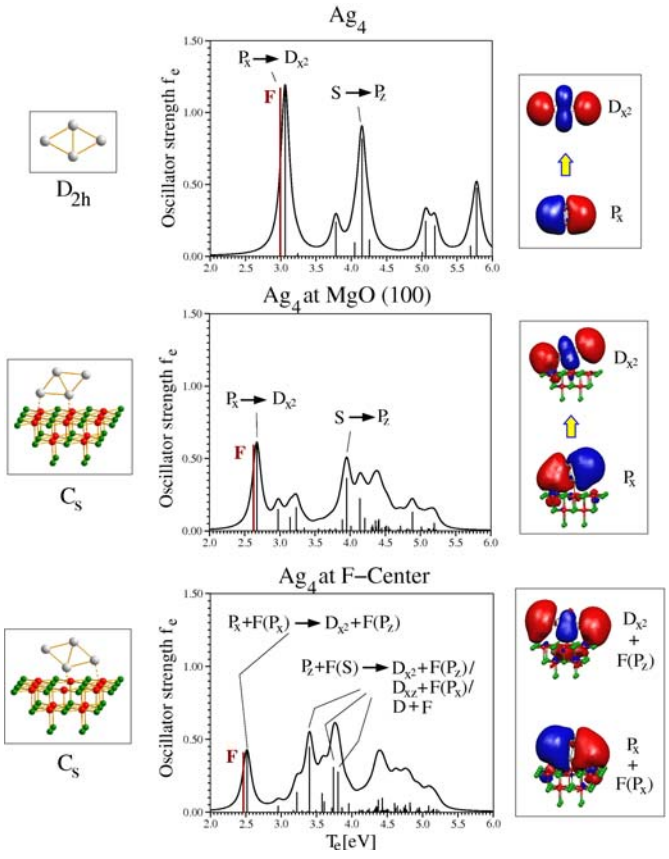

Fig. 3. (Color online) Comparison of absorption spectra for free Ag_4, Ag_4 at stoichiometric MgO(100) and Ag_4 at F_S-center defect obtained for optimized structures. The nature of characteristic excitations involved in intense transitions are assigned and the corresponding orbitals are shown. The position of the fluorescence line (red line) obtained by optimizing the geometry of the corresponding excited state is labeled by F.

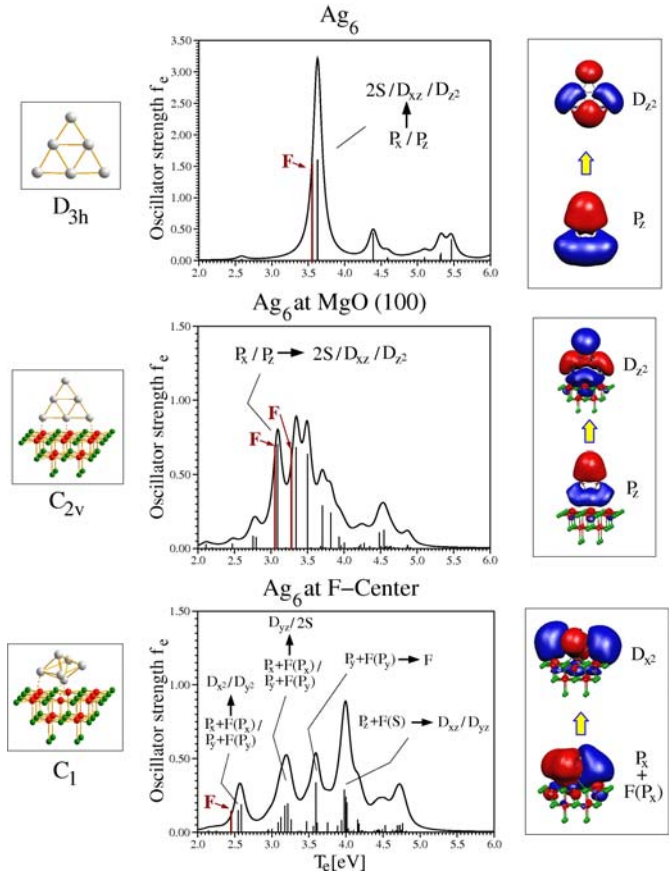

Fig. 4. (Color online) Comparison of absorption spectra for free Ag_6, Ag_6 at stoichiometric MgO(100) and Ag_6 at F_S-center defect obtained for optimized structures. The nature of characteristic excitations involved in intense transitions are assigned and the corresponding orbitals are shown. The position of the fluorescence line (red line) obtained by optimizing the geometry of the corresponding excited state is labeled by F.

transitions and therefore the Ag_4 at F_S-defect is also a good candidate for an emissive center in the visible range. It is interesting to emphasize that different nature of interaction with different sites of the support (polarization at surface versus F_S-center) gives rise to intense transitions in the similar spectral regions, but the nature of excitations leading to these intense transitions is intrinsically different.

Ag_6/MgO

In contrast to the previous cases Ag_6 assumes different structures at different support sites. In the case of stoichiometric surface planar Ag_6 is perpendicularly bound to the support while Ag_6 assumes 3D bipyramidal structure at F_S-defect (cf. Fig. 4). These structural properties influence strongly spectroscopic patterns as can be seen from Figure 4. In the case of Ag_6 at stoichiometric support the occupied P_x- and P_z-type orbitals are almost degenerate due to similar sizes of x- and z-dimension of the cluster while P_y orbital remains unoccupied and lies higher in energy. Consequently, the transitions located at 3.09 and 3.34 eV are reminiscent from doubly degenerate transition in free Ag_6 cluster. In fact, the transition at 3.09 eV is dominated by combination of the excitations $P_x \rightarrow 2S$, $P_x \rightarrow D_{z^2}$ and $P_z \rightarrow D_{xz}$. The transition of 3.34 eV is of similar nature with additional contribution of excitation from P_z to the linear combination of S-type cluster plus surface orbitals. The red shift of these transitions in supported clusters is due to the polarization by the surface. The third intense transition at 3.50 eV arises mainly by excitations from P_z to linear combination of 2S-type cluster plus surface orbitals and is inherent to supported Ag_6 cluster. Notice, that in the case of Ag_6 at stoichiometric surface the fluorescence from described intense transitions might in principle take place but there are several low lying excited states which might influence emission process.

The absorption pattern of Ag_6 at F_S-defect shown in Figure 4 exhibits completely different features due to 3D structure in which four atoms are directly interacting with the support. Therefore, there is a similarity between spectroscopic patterns of Ag_4 at F_S-defect and Ag_6 at F_S-defect. In the latter case the lowering of the symmetry causes the splitting of the lowest energy transitions located at 2.55 and 2.59 eV. Since six valence electrons

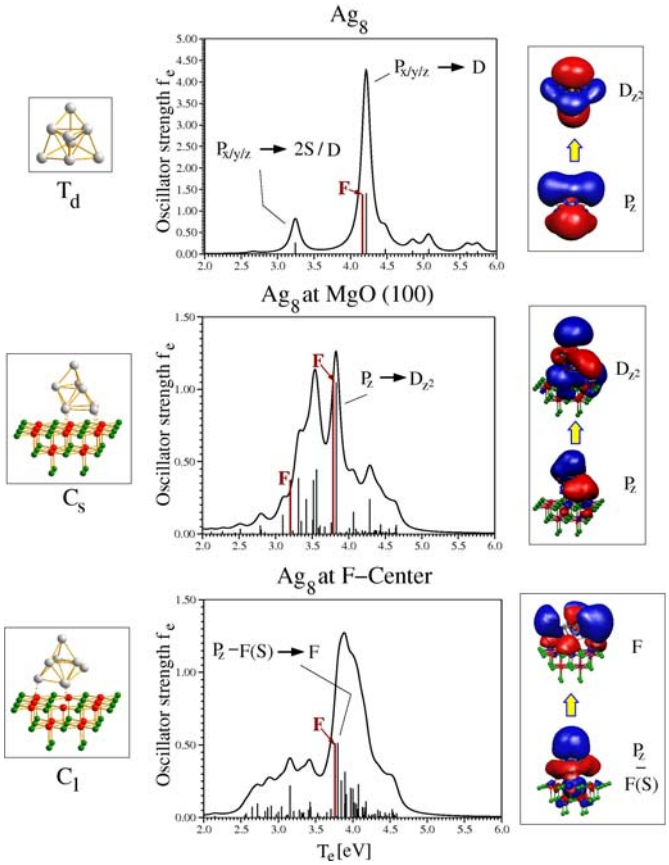

Fig. 5. (Color online) Comparison of absorption spectra for free Ag_8, Ag_8 at stoichiometric MgO(100) and Ag_8 at F_S-center defect obtained for optimized structures. The nature of characteristic excitations involved in intense transitions are assigned and the corresponding orbitals are shown. The position of the fluorescence line (red line) obtained by optimizing the geometry of the corresponding excited state is labeled by F.

of Ag_6 occupy two close lying P_y + $F(P_y)$ and P_x + $F(P_x)$ orbitals and the P_z + F(S) orbital, the two lowest energy transitions at 2.55 and 2.59 eV arise from P_y + $F(P_y)$ → D_{y^2} and P_x + $F(P_x)$ → D_{x^2} excitations. Higher lying transitions around 4 eV are dominated by excitations from HOMO-2, which is of P_z + F(S) type, to corresponding symmetry allowed orbitals. The red shift of the two lowest energy intense transitions with respect to the dominant transition in the free cluster is caused by the contribution from the F_S-center. As already mentioned due to geometric deformation of Ag_6 and the contribution of the F_S-center the emission is expected in the visible regime.

Ag_8/MgO

The three-dimensionality of supported Ag_8 cluster with filled S- and P-type valence orbitals gives rise to absorption patterns with dominant transitions distributed in large energy interval as shown in Figure 5. In the case of Ag_8 at stoichiometric surface the dominant transitions are located in the energy interval of 3.4 to 3.5 eV and 3.8 eV. The excitations giving rise to intense transitions are of P → D type. The splitting of intensities is due to the lowering of symmetry with respect to the gas phase Ag_8 T_d structure. The polarization by the surface causes again the red shift of the spectroscopic pattern of supported cluster. The close position of the fluorescence bands to the intense absorption transitions for selected excited states indicate that emission might be observed in broad energy range. However, the increased density of low lying excited states can substantially influence emissive properties.

For Ag_8 at the F_S-center the P_z – F(S) (D-type) orbital becomes HOMO. Therefore, large number of D → F type excitations contribute to the intense transitions which are spread in the energy interval between 2.5 and 3.5 eV and above 3.75 eV, as shown in Figure 5. The spectroscopic pattern of Ag_8 at the F_S-center can be considered to arise from the spectroscopic pattern of Ag_6 at the F_S-center by superposing additional excitations from the HOMO to the F-type orbitals. The distinct feature of Ag_8 at F_S-center is that no separated intense transitions in visible regime are present as it is the case for smaller clusters. Therefore, it is to expect that different emissive properties will arise. The determination of the lifetimes of electronic states would be necessary to predict the possible occurrence of fluorescence. It is interesting to notice that in spite of the discrete energy levels, the spectroscopic pattern of supported Ag_8 already resembles to those expected for larger nanoparticles.

4 Summary and outlook

The above described results show that absorption and emission properties of small silver clusters at the MgO support can be tuned by the cluster size, cluster structure and the site of the support. The inherent characteristic features of the absorption of free clusters remain to large extent preserved in the case of the stoichiometric site. Some of intense transitions involving excitations among orbitals which are polarized by the surface are red shifted with respect to those in free clusters in spite of the weak interaction between the cluster and the stoichiometric site. However, the location of intense absorption and fluorescence bands in the visible regime is present only for Ag_4 at MgO(100). The fluorescence in the higher energy intervals for other supported cluster sizes cannot be excluded but the determination of lifetimes would be desirable in order to predict the efficiency of those emissive centers.

The interaction between the cluster and the F_S-center can be qualitatively understood on the basis of four orbitals which arise from combination of F_S-center S-orbital with three cluster P-type orbitals which give rise to one P_z + F(S) orbital, two degenerate P_x + $F(P_x)$ and P_y + $F(P_y)$ orbitals, and the antibonding P_z – F(S) orbital which are sequentially filled by electrons by increasing the cluster size. The excitations from these orbitals to higher unoccupied orbital types with appropriate symmetry give rise to characteristics of intense transitions. Therefore, the analysis of excitations allow us to classify

three types of excitations. The first type involves excitations closely related to those found in the free clusters as it has been identified in the case of Ag_4 and Ag_6 at the F_S-center. The second type of excitations are due to the F_S-center and are characteristic for two lowest intense transitions in Ag_2 at F_S-center. The third type of excitations characterized by strong mixing of excitations within the cluster and the F_S-center have been identified for Ag_8 at F_S-center. The above classification allowed us to unravel the mechanism responsible for optical properties of silver clusters at F_S-defect. Our findings indicate that Ag_n ($n = 2, 4, 6$) at the F_S-center are good candidates for the emissive centers in the visible energy range below 2.5 eV. By adding only two atoms in Ag_8 similarities with absorption properties of larger nanoparticles have been recognized. Therefore, the future investigation should be focused in three directions. First, the influence of further increasing the cluster size on the new characteristic features of absorption patterns should be established. The connection between the nature of filled cluster-support-site orbitals from which excitations could take place and the absorption patterns should provide basis for development of functionalized supported clusters. Secondly, the absorption properties of silver clusters at other MgO defects should be investigated. Third, the interplay between the lifetimes of excited states with the size and the structure of supported clusters has to be explored in order to determine the efficiency of emissive centers.

We gratefully acknowledge financial support by the Deutsche Forschungsgemeinschaft priority program SPP 1153 "Clusters at Surfaces: Electron Structure and Magnetism".

References

1. L.A. Peyser, A.E. Vinson, A.P. Bartko, R.M. Dickson, Science **291**, 103 (2001)
2. J. Zheng, R.M. Dickson, J. Am. Chem. Soc. **124**, 13982 (2002)
3. J. Zheng, J.T. Petty, R.M. Dickson, J. Am. Chem. Soc. **125**, 7780 (2003)
4. T.H. Lee, R.M. Dickson, PNAS **100**, 3043 (2003)
5. T.H. Lee, R.M. Dickson, J. Phys. Chem. B **107**, 7387 (2003)
6. T. Gleitsmann, B. Stegemann, T.M. Bernhardt, Appl. Phys. Lett. **84**, 4050 (2004)
7. T.H. Lee, J.I. González, J. Zheng, R.M. Dickson, Acc. Chem. Res. **38**, 534 (2005)
8. T. Gleitsmann, T.M. Bernhardt, L. Wöste, Appl. Phys. A **82**, 125 (2006)
9. E. Katz, I. Willner, Angew. Chem., Int. Ed. **43**, 6042 (2004)
10. L. Peyser-Capadona, J. Zheng, J.I. González, T.H. Lee, S.A. Patel, R.M. Dickson, Phys. Rev. Lett. **94**, 058301 (2005)
11. L. König, I. Rabin, W. Schulze, G. Ertl, Science **274**, 1353 (1996)
12. I. Rabin, W. Schulze, G. Ertl, J. Chem. Phys. **108**, 5137 (1998)
13. I. Rabin, W. Schulze, G. Ertl, C. Félix, C. Sieber, W. Harbich, J. Buttet, Chem. Phys. Lett. **320**, 59 (2000)
14. C. Félix, C. Sieber, W. Harbich, J. Buttet, I. Rabin, W. Schulze, G. Ertl, Phys. Rev. Lett. **86**, 2992 (2001)
15. C. Sieber, J. Buttet, W. Harbich, C. Félix, R. Mitrić, V. Bonačić-Koutecký, Phys. Rev. A **70**, 041201 (2004)
16. T. Diederich, J. Tiggesbäumker, K.H. Meiwes-Broer, J. Chem. Phys. **116**, 3263 (2002)
17. V. Bonačić-Koutecký, J. Pittner, M. Boiron, P. Fantucci, J. Chem. Phys. **110**, 3876 (1999)
18. V. Bonačić-Koutecký, V. Veyret, R. Mitrić, J. Chem. Phys. **115**, 10450 (2001)
19. C. Bürgel, R. Mitrić, V. Bonačić-Koutecký, Appl. Phys. A **82**, 117 (2006)
20. B. Yoon, H. Häkkinen, U. Landman, A.S. Wörz, J.M. Antonietti, S. Abbet, K. Judai, U. Heiz, Science **307**, 403 (2005)
21. D. Ricci, C. Di Valentin, G. Pacchioni, P. Sushko, A. Shluger, E. Giamello, J. Am. Chem. Soc. **125**, 738 (2003)
22. M. Chiesa, M. Paganini, E. Giamello, D. Murphy, C. DiValentin, G. Pacchioni, Acc. Chem. Res. **39**, 861 (2006)
23. M. Sterrer, M. Heyde, M. Novicki, N. Nilius, T. Risse, H.P. Rust, G. Pacchioni, H.J. Freund, J. Phys. Chem. B **110**, 46 (2006)
24. C. Inntam, L.V. Moskaleva, I.V. Yudanov, K.M. Neyman, N. Rösch, Chem. Phys. Lett. **417**, 515 (2006)
25. C. Inntam, L.V. Moskaleva, K.M. Neyman, V.A. Nasluzov, N. Rösch, Appl. Phys. A **82**, 181 (2006)
26. G. Barcaro, A. Fortunelli, J. Chem. Theory Comput. **1**, 972 (2005)
27. L. Giordano, M. Baistrocchi, G. Pacchioni, Phys. Rev. B **72**, 115403 (2005)
28. K.M. Neyman, C. Inntam, V.A. Nasluzov, R. Kosarev, N. Rösch, Appl. Phys. A **78**, 823 (2004)
29. K.M. Neyman, C. Inntam, A.V. Matveev, V.A. Nasluzov, N. Rösch, J. Am. Chem. Soc. **127**, 11652 (2005)
30. A. Bogicevic, D.R. Jennison, Surf. Sci. **515**, L481 (2002)
31. A.V. Matveev, K.M. Neyman, I.V. Chudanov, N. Rösch, Surf. Sci. **426**, 123 (1999)
32. A.M. Ferrari, C. Xiao, K.M. Neyman, G. Pacchioni, N. Rösch, Phys. Chem. Chem. Phys. **1**, 4655 (1999)
33. A.V. Matveev, K.M. Neyman, G. Pacchioni, N. Rösch, Chem. Phys. Lett. **299**, 603 (1999)
34. I. Yudanov, G. Pacchioni, K.M. Neyman, N. Rösch, J. Phys. Chem. B **101**, 2786 (1997)
35. A.M. Ferrari, G. Pacchioni, J. Phys. Chem. **100**, 9032 (1996)
36. M. Walter, H. Häkkinen, Phys. Rev. B **72**, 205440 (2005)
37. A. del Vitto, C. Sousa, F. Illas, G. Pacchioni, J. Chem. Phys. **121**, 7457 (2004)
38. G. Pacchioni, P.S. Bagus, F. Parmigiani, *Cluster Models for Surface and Bulk Phenomena*, NATO ASI Series B (Plenum, New York, 1992), Vol. 283
39. M.A. Nygren, L.G.M. Pettersson, Z. Barandiarán, L. Sejio, J. Chem. Phys. **100**, 2010 (1994)
40. N.W. Winter, R.M. Pitzer, J. Chem. Phys. **89**, 446 (1988)
41. J.A. Mejías, A.M. Márquez, M. Fernández-Sanz, J.M. Ricart, C. Sousa, F. Illas, Surf. Sci. **327**, 59 (1995)
42. J.P. Perdew, K. Burke, M. Ernzerhof, Phys. Rev. Lett. **77**, 3865 (1996)
43. D. Andrae, U. Haeussermann, M. Dolg, H. Stoll, H. Preuss, Theor. Chim. Acta **77**, 123 (1990)
44. D. Peterka, C. Tegenkampf, K.M. Schröder, W. Ernst, H. Pfnür, Surf. Sci. **431**, 146 (1999)
45. F. Illas, G. Pacchioni, J. Chem. Phys. **108**, 7835 (1998)